Renewable Energy and Power Quality Journal
https://repqj.com/index.php/repqj/index
RE&PQJ, Vol. 24, No. 1, 2026

Comparative Analysis of Single-Phase Shift and Extended Phase Shift Modulations in Dual Active Bridge Converters for Fast EV Charging

Mohamed R. Farid [1, 2] *, Ahmed L. Elrefai [1, 3] and Sobhy M. Abdelkader [1, 4]

[1] Electrical Power Engineering Department, Faculty of Engineering, Egypt-Japan University of Science and Technology (E-JUST), New Borg El Arab City, Alexandria 21934, Egypt
[2] Electrical Engineering Department, Benha Faculty of Engineering, Benha University, Benha 13518, Egypt
[3] Electrical Power Engineering Department, Cairo University, Giza 12613, Egypt
[4] Electrical Engineering Department, Mansoura University, El-Mansoura 35516, Egypt
* Corresponding Author: Tel: (+2) 01069560387. E-mail: mohamed.abdelrhman@ejust.edu.eg

Abstract. This paper presents a comprehensive comparison between Single-Phase Shift Modulation (SPSM) and Extended Phase Shift Modulation (EPSM) in Dual Active Bridge (DAB) converters, focusing on their switching losses, performance, and efficiency under various load conditions. The analysis is conducted using SPICE-based simulations to evaluate the converters' behaviour under low, medium, and high-loading conditions. The DAB converter is designed for fast-charging electric vehicle (EV) applications with the design specifications of 5 kW, 800V/400V employing Silicon Carbide (SiC) MOSFETs with switching frequency of 100 kHz. The comprehensive comparative analysis of the two modulation strategies yields critical insights regarding their appropriateness for various applications and operational scenarios, which is fundamental to achieving efficient high-power DC-DC conversion in advanced electric vehicle fast charging systems.

Key words. EV fast charging, DAB, Silicon carbide devices, Single Phase Shift, Extended Phase Shift.

Introduction

The increasing adoption of electric vehicles (EVs) necessitates the development of efficient and high-power charging solutions to minimize charging times and enhance user convenience [1]. Among the various power conversion topologies, the Dual Active Bridge (DAB) converter has emerged as a highly promising candidate for fast-charging applications, owing to its high efficiency and bidirectional power transfer capability, which supports both grid-to-vehicle (G2V) and vehicle-to-grid (V2G) operations [2]. Additionally, the DAB topology plays a key role in advanced energy management strategies, contributing to improved grid stability. The converter also enables soft-switching operation, i.e. zero-voltage switching (ZVS) and zero-current switching (ZCS) [3], which significantly reduce switching losses. This reduction enhances overall power conversion efficiency and minimizes thermal stress, both of which are critical for the reliability and performance of high-power fast-charging systems.

Although the DAB converter offers numerous advantages, its performance is highly dependent on the modulation technique and operating conditions. Additionally, variations in loading conditions, which are common in fast-charging applications where battery voltage changes during the charging process, can significantly impact power conversion efficiency and overall system stability [4]. Therefore, selecting an optimal modulation technique and implementing adaptive control strategies based on real-time operating conditions are crucial for maximizing the DAB converter's effectiveness in high-power EV fast-charging applications. The modulation strategies of single phase shift modulation (SPSM) and extended phase shift modulation (EPSM) directly influence the overall efficiency, power transfer capability, and soft-switching range of the DAB converter. While SPSM is widely used due to its simplicity, it suffers from limited ZVS at light loads. On the other hand, EPSM enhances performance by dynamically adjusting phase shifts to extend the ZVS range and reduce circulating current losses, making it more efficient under varying loading conditions.

This paper investigates the performance characteristics of 5 kW, 800V/400V, 100 kHz DAB converter using Silicon-Carbide (SiC) MOSFETs for fast-charging electric vehicle EV applications. The comparative study of SPSM and EPSM under different loading conditions provides valuable insights into their impact on minimizing losses, improving thermal management, and enhancing overall system reliability. Evaluating these modulation strategies across low, medium, and high loading levels is essential for optimizing high-power DC-DC conversion in next-generation EV fast chargers for appropriate use of each modulation technique to minimize switching losses and efficiently operate of the DAB converter in different applications and loading conditions.

1. DAB Converter Operation

A single-phase Dual Active Bridge DAB converter consists of two full-bridge inverters connected through a high-frequency transformer as shown in Fig. (1). The power transfer between the two bridges is controlled by adjusting the phase shift between their switching signals.

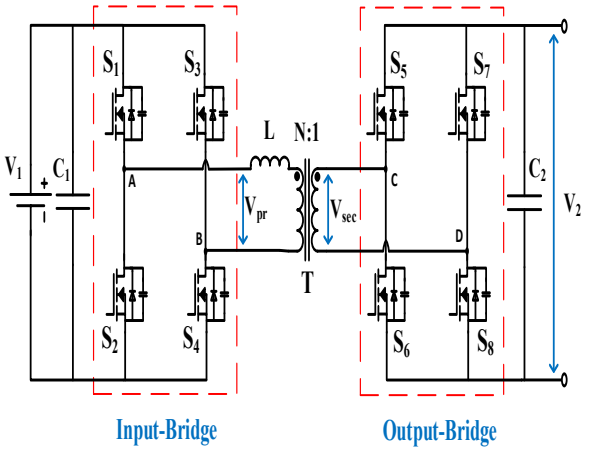

Fig. 1. The structure of a single-phase DAB converter

In a DAB converter, power transmission at high frequencies can be resembled by the behaviour of a sinusoidal AC power system, where the transmitted power is determined by the phase difference between AC voltage V_{pr} and $V_{\sec}$. Mathematically, it can be expressed as follows [5]:

$$P = \frac{\boldsymbol{V_{pr-rms}V_{sec-rms}}}{2\pi fL} sin(\phi) \qquad (1)$$

where V_{pr-rms} and $V_{\sec-rms}$ are the RMS values of V_{pr} and $V_{\sec}$ respectively, f is the fundamental switching frequency, L represents the transformer's leakage inductance, and ϕ is the phase shift between the two voltage waveforms. When sinusoidal sources are replaced with square pulsating voltage waveforms. the power transfer mechanism remains similar, the transmitted power in a DAB converter can be deduced to be given by [5]:

$$P = \frac{NV_1V_2}{2\pi^2 fL}\phi(\pi - |\phi|) \qquad (2)$$

where *V1* and *V2* are the DC voltages 1 and 2, respectively. To simplify the power equation, we introduce a normalized phase shift ratio, δ, defined as: $\delta = \frac{\phi}{\pi}$, The expression now explicitly shows that power depends on δ as follows [4]:

$$P_{SPSM} = \frac{NV_1V_2}{2fL}\delta(1 - |\delta|) \qquad (3)$$

Table 1 outlines the system specifications, including input and output voltage levels, power rating, output power, switching frequency, transformer turns ratio, leakage inductance, and the part numbers of the used SiC MOSFETs and Diodes. These specifications were designed to ensure high efficiency, minimal losses, and optimal performance in fast-charging EV applications. The parameters of Table I were used to construct the DAB converter model on LTSPICE. The results from the constructed model are used to evaluate the DAB performance while implementing SPSM and EPSM modulation techniques for the operation of the DAB converter.

Table I.- system parameters

Parameter	Symbol	Value
Input DC Voltage	V_1	800 V
Output DC Voltage	V_2	400 V
Switching Frequency	f	100 kHz
Transformer Ratio	N	2:1
Leakage inductance	L	160 µH
Output Power	P	5 KW
Primary SiC MOSFET (C3M0075120J)	V_{DS}	1200 V
	I_D	30 A at T_C = 25°C 19.7 A at T_C=100°C
	R_{DS}	75 mΩ
Primary SiC DIODE (C4D30120D)	V_{PRV}	1200 V
	I_F	44 A at T_C = 25°C 30 A at T_C =152°C
Secondary SiC MOSFET (C3M0060065K)	V_{DS}	650 V
	I_D	37 A at TJ = 25°C 27 A at TJ = 100°C
	R_{DS}	60 mΩ
Secondary SiC DIODE (C6D30065H)	V_{PRV}	650 V
	I_F	44A at T_C = 25°C 27A at T_C =150°C

A. SINGLE-PHASE SHIFT MODULATION

Single-Phase Shift control is the most fundamental and widely used modulation strategy for DAB converters. In this method, both the primary and secondary full bridges operate with a fixed 50% duty cycle, and power transfer is regulated by introducing a phase shift between their switching waveforms, by adjusting this phase shift, the direction and magnitude of power flow can be controlled. Power transfer is maximized when the phase shift is at ($\phi = \pi/2$). At this point, the system operates at its highest power delivery capability and the power delivered can be calculated using Eq (4), Noted that at ($\phi = \pi/2$), DAB will be transferring the highest power to the output-bridge, however, it also experiences increased circulating currents, which may lead to higher conduction losses [4].

$$P_{SPS(max)} = \frac{NV_1V_2}{8fL} \qquad (4)$$

B. EXTENDED-PHASE SHIFT MODULATION

Unlike SPSM, which applies a single-phase shift between the two bridges, EPSM introduces an additional inner phase shift (δ_{in}) between the diagonal switches of each individual bridge, alongside the outer phase shift (δ_{out}) between the input-bridge and output-bridge. This dual-phase shift approach allows for improved efficiency and reduced current peaks, particularly in applications with varying load condition. Extended Phase Shift modulation EPSM enhances the performance of the DAB converter by providing a wider ZVS range at medium loading conditions, reducing backflow power, and minimizing current stress compared to SPSM. The power transfer equation under EPSM is given as follows [4]:

$$P_{EPSM} = \frac{NV_1V_2}{4fL}[\delta_{in}(1 - \delta_{in} - 2\delta) + 2\delta(1 - \delta)] \qquad (5)$$

While EPSM improves ZVS range and reduces backflow power, it does not increase the overall power transfer capability of the DAB converter since the maximum transferable power in EPSM is equal to that in SPSM as follows [4]:

$$P_{EPSM(max)} = P_{SPSM(max)} = \frac{NV_1V_2}{8fL} \quad (6)$$

2. Simulation and Discussion

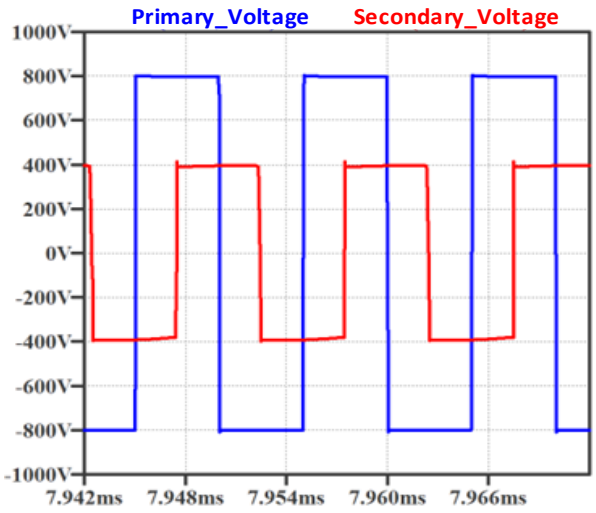

Fig. 2. Primary and Secondary Voltage Waveforms of SPSM at nominal loading condition of 5 kW

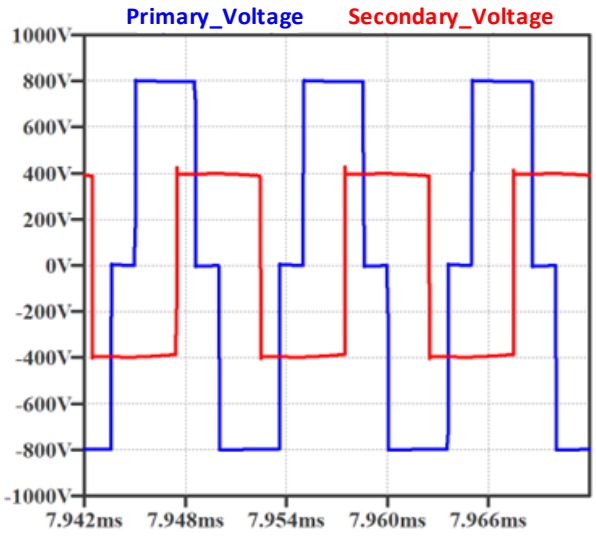

Fig. 3. Primary and Secondary Voltage Waveforms of EPSM at nominal loading condition of 5 kW

The primary voltage V_{pr} and secondary voltage V_{sec} at nominal loading condition of 5 kW for the modulation techniques SPSM and EPSM are shown in Fig. (2) and Fig. (3), respectively. Fig. (4) and Fig. (5) show the inductor's voltages and currents of SPSM and EPSM at same loading condition. The comparative performance of SPSM and EPSM topologies is illustrated in Figs. (6) to (12), focusing on efficiency and power losses across a wide range of output power levels. Fig. (6) shows that EPSM consistently outperforms SPSM in terms of efficiency, particularly under medium and full load conditions. The peak efficiency of EPSM reaches 98.23%, outperforming SPSM by up to 0.95 in relative efficiency under medium and full load conditions, compared to the maximum efficiency of 97.31% achieved by SPSM. At light output power levels (around 1.2 kW), EPSM maintains an efficiency of 96.76%, compared to 94.59% for SPSM, indicating a relative improvement of almost 2.3% in light-load scenarios.

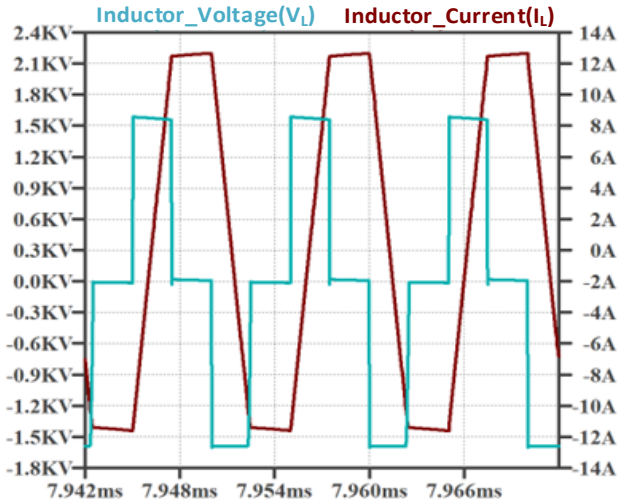

Fig. 4. Inductor Voltage and Current Waveforms of SPSM at nominal loading condition of 5 kW

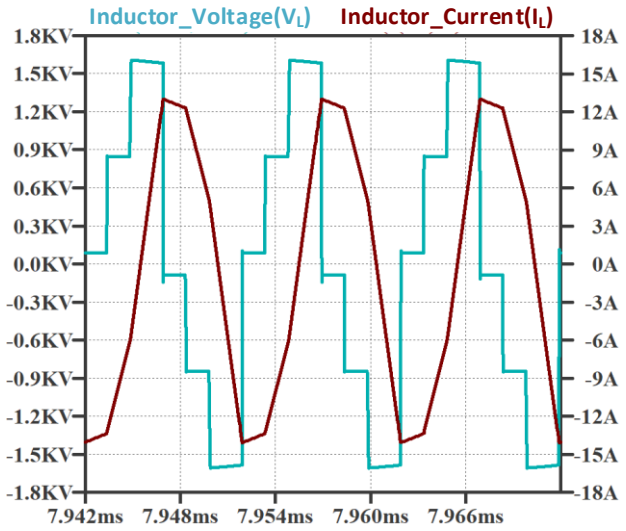

Fig. 5. Inductor Voltage and Current Waveforms of EPSM at nominal loading condition of 5 kW

Fig. (7) and Fig. (8) demonstrate the resulted switching losses in the MOSFETs of *S1* and *S5* in the primary and secondary sides, respectively. In both cases, EPSM exhibits significantly lower switching losses. the primary-side switching loss at full load is reduced from 21.14 W in SPSM to 6.80 W in EPSM which corresponds to around 67.8% reduction. Similarly, the secondary-side MOSFET losses show a decrease from 12.54 W in SPSM to 11.01 W in EPSM. According to diode conduction losses, Fig. (9) and Fig. (10) display the losses in the upper left diode in

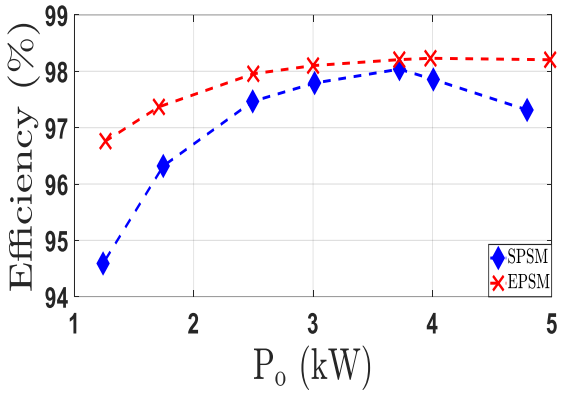

Fig. 6. Overall Efficiency between SPSM and EPSM under different loading conditions

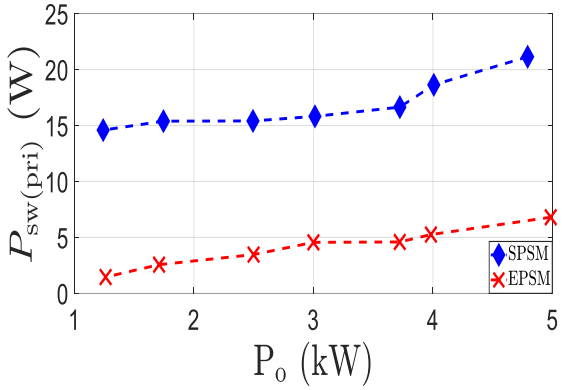

Fig. 7. Primary-side *S1* MOSFET losses for SPSM and EPSM under different loading conditions

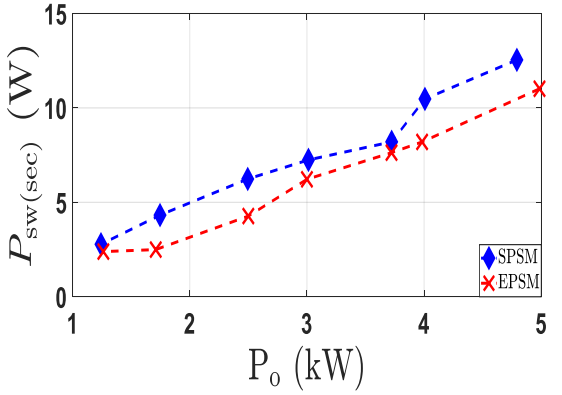

Fig. 8. Secondary-side *S5* MOSFET losses for SPSM and EPSM under different loading conditions

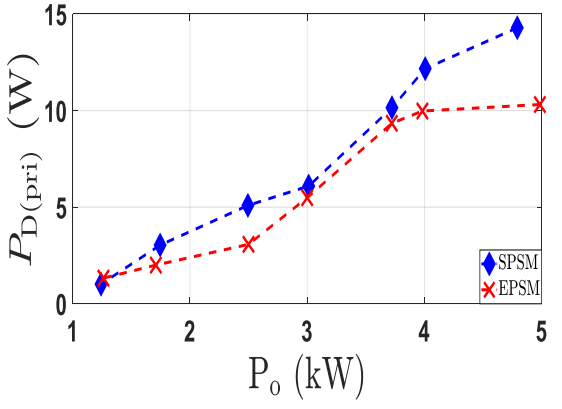

Fig. 9. Primary-side *S1* diode losses for SPSM and EPSM under different loading conditions

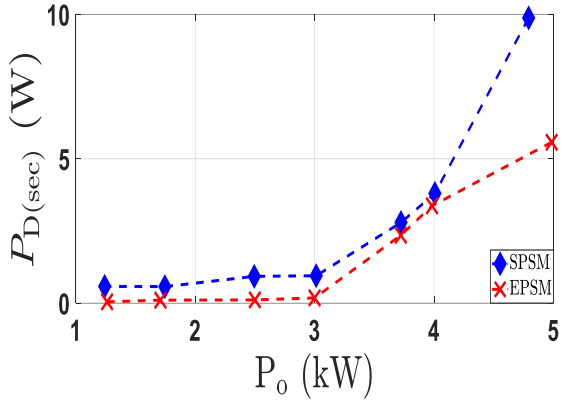

Fig. 10. Secondary -side *S5* diode losses for SPSM and EPSM under different loading conditions

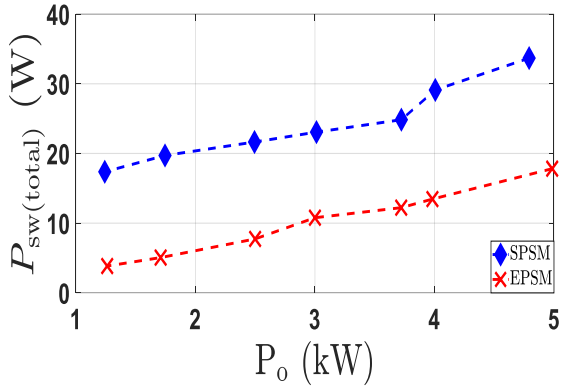

Fig. 11. Total MOSFET losses for SPSM and EPSM under different loading conditions

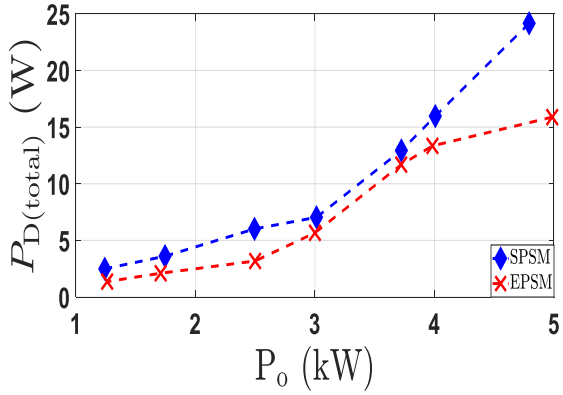

Fig. 12. Total diode losses for SPSM and EPSM under different loading conditions

the primary and secondary bridges, respectively. EPSM achieves a reduction in primary diode losses, from 14.28 W in SPSM to 10.31 W in EPSM at high loading levels with about 27.8% decrease. Even more notable is the secondary diode loss, which drops from 9.88 W in SPSM to 5.57 W in EPSM under the same conditions, yielding a roughly 43.6% reduction. Fig. (11) shows total MOSFET losses, where EPSM outperforms SPSM across all power levels. At nominal output power, EPSM reduces total MOSFET losses from 33.68 W to 17.82 W, representing a 47.1% decrease. This consistent gap highlights the superior switching behavior of EPSM due to its soft-switching nature. Finally, Fig. (12) illustrates the total diode losses, where EPSM demonstrates a clear advantage, achieving a total loss of 15.88 W at full load compared to 24.16 W in SPSM, equivalent to a nearly 34.3% reduction.

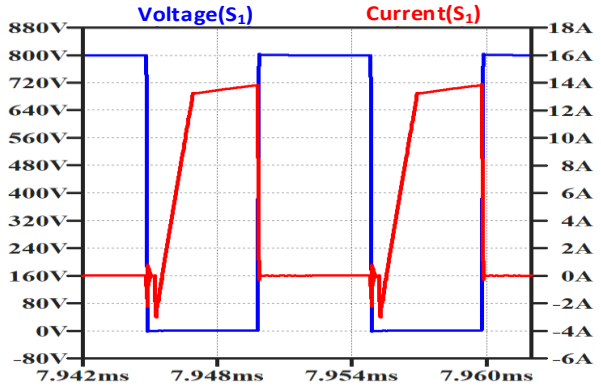

Fig. 13 Primary-side S1 ZVS Waveforms of SPSM at nominal loading condition of 5 kW

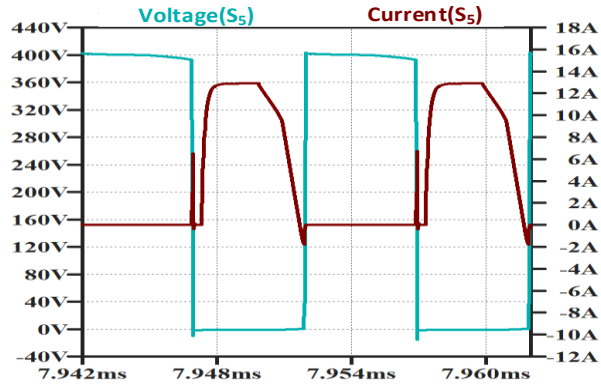

Fig. 14 Secondary-side S5 ZVS Waveforms of SPSM at nominal loading condition of 5 kW

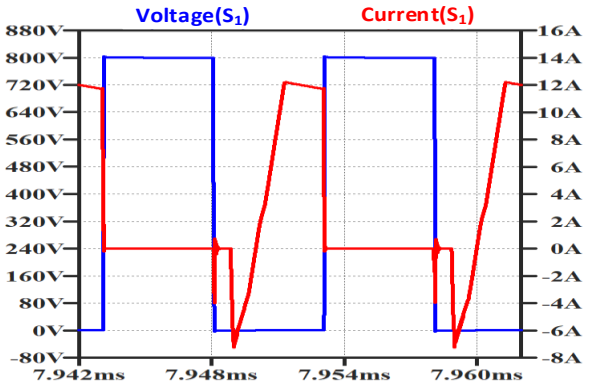

Fig. 15 Primary-side S1 ZVS Waveforms of EPSM at nominal loading condition of 5 kW

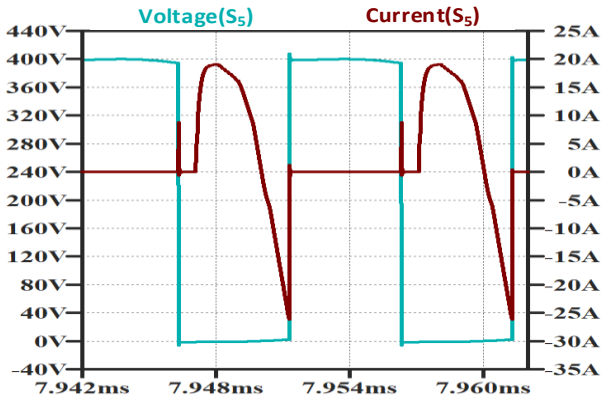

Fig. 16 Secondary-side S5 ZVS Waveforms of EPSM at nominal loading condition of 5 kW

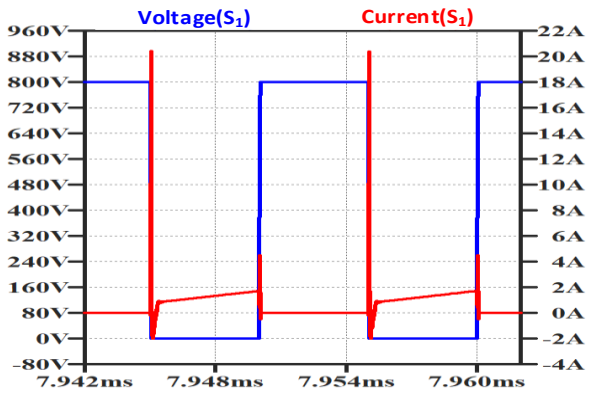

Fig. 17 Primary-side S1 hard switching Waveforms of SPSM at light loading condition of 1.25 kW

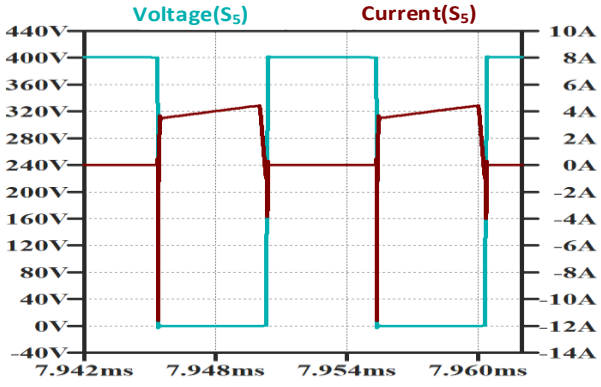

Fig. 18 Secondary-side S5 hard switching Waveforms of SPSM at light loading condition of 1.25 kW

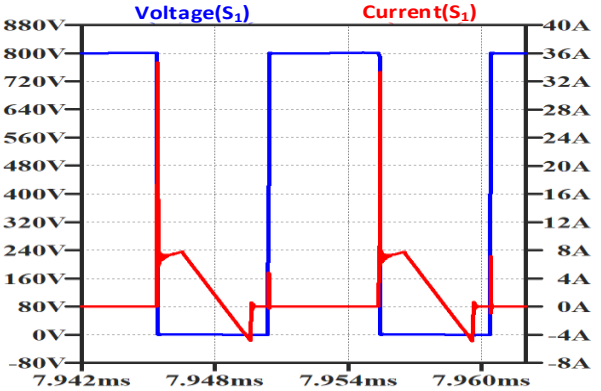

Fig. 19 Primary-side S1 ZCS Waveforms of EPSM at light loading condition of 1.25 kW

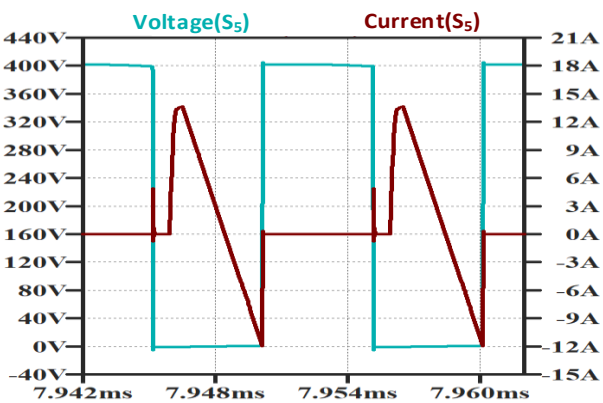

Fig. 20 Secondary-side S5 ZVS Waveforms of EPSM at light loading condition of 1.25 kW

The results presented in the Figures 13–16 compare ZVS performance in a DAB converter using SPSM and EPSM at 5 kW nominal load. While both achieve soft switching, EPSM provides better ZVS due to its flexible control of phase shifts. In contrast, SPSM loses ZVS under light-load conditions at 1.25 kW, resulting in hard-switching behaviour due to insufficient current overlap during switching transitions, as shown in Figures 17–20. Meanwhile, EPSM maintains soft switching across the switches, even at reduced load levels, thanks to its ability to independently adjust the phase shifts of the primary and secondary bridges. This control enables sufficient circulating current to sustain Zero Voltage Switching (ZVS) despite the lower power transfer. The investigation results for both modulation techniques are summarized in Table II.

Table II.- Performance Comparison of (SPSM) and (EPSM) in a DAB Converter [4],[6].

Parameter	SPSM	EPSM
Switching Losses	Higher switching losses due to limited ZVS range, especially at light loads.	Reduced switching losses as EPSM provides a wider ZVS range, particularly at medium power levels.
Load Variation	Performance is optimal at nominal power but deteriorates at varying loads.	More adaptable to load variations due to additional control flexibility
Efficiency	Lower efficiency at light and medium loads due to increased losses.	Higher efficiency across different load conditions due to reduced backflow power and better ZVS utilization.

The findings presented in Table II highlight that SPSM performs well in nominal conditions, while EPSM demonstrates higher efficiency at medium and light loads due to occurrence of ZVS, reduction of switching losses, and minimization of circulating currents. This highlights that EPSM is considered more optimal for high-power applications with wide load variations, while SPSM gives optimal performance at nominal loading condition.

Conclusion

This paper presents a comparative investigation under varying loading conditions for the performance of single-phase-shift and extended-phase-shift modulation techniques for a Dual Active Bridge (DAB) converter implemented with SiC MOSFETS and designed for fast-charging electric vehicles with the ratings of 5 kW, 800V/400V and 100 kHz. The findings indicate that SPSM has optimal performance only under nominal rated conditions. However, under varying loading condition, EPSM offers superior performance by reducing switching losses and confirms a consistent efficiency improvement of approximately 0.5%-2.1% with its ability to lower backflow power and expand the zero-voltage switching (ZVS) range. These benefits establish EPSM, in combination with SiC-based power devices, as an optimal solution for next-generation fast-charging systems, enabling faster and more efficient EV charging.

References:

[1] M. Safayatullah, M. T. Elrais, S. Ghosh, R. Rezaii, and I. Batarseh, “A Comprehensive Review of Power Converter Topologies and Control Methods for Electric Vehicle Fast Charging Applications,” *IEEE Access*, vol. 10, pp. 40753–40793, 2022, doi: 10.1109/ACCESS.2022.3166935.

[2] F. S. Zehgeer, A. Haque, S. Mateen, and N. Shah, “Review of the Isolated Dual Active Bridge Converter Topologies for the Fast and Ultra-Fast Charging of Electric Vehicles,” in *2023 11th National Power Electronics Conference (NPEC)*, Dec. 2023, pp. 1–6. doi: 10.1109/NPEC57805.2023.10384974.

[3] E. L. Carvalho *et al.*, “Extended ZVS-On/ZCS-Off Range for CF-DAB Converter Under DCM Operation for Residential Energy Storage Systems,” *IEEE Access*, vol. 11, pp. 119231–119243, 2023, doi: 10.1109/ACCESS.2023.3327219.

[4] N. Noroozi, A. Emadi, and M. Narimani, “Performance Evaluation of Modulation Techniques in Single-Phase Dual Active Bridge Converters,” *IEEE Open J. Ind. Electron. Soc.*, vol. 2, pp. 410–427, 2021, doi: 10.1109/OJIES.2021.3087418.

[5] B. Zhao, Q. Song, W. Liu, and Y. Sun, “Overview of Dual-Active-Bridge Isolated Bidirectional DC–DC Converter for High-Frequency-Link Power-Conversion System,” *IEEE Trans. Power Electron.*, vol. 29, no. 8, pp. 4091–4106, Aug. 2014, doi: 10.1109/TPEL.2013.2289913.

[6] F. Xu, J. Liu, and Z. Dong, “Minimum Backflow Power and ZVS Design for Dual-Active-Bridge DC–DC Converters,” *IEEE Trans. Ind. Electron.*, vol. 70, no. 1, pp. 474–484, Jan. 2023, doi: 10.1109/TIE.2022.3156159.